



Research Article

# Effect of aerogel/silica fume under curing methods on properties of cement-based mortars

Ozlem Ustundag<sup>1\*</sup>, Ozlem Celik Sola<sup>2</sup>

<sup>1</sup> Istanbul University-Cerrahpasa, Department of Civil Engineering, Istanbul (Türkiye), [ozlem.ustundag@iuc.edu.tr](mailto:ozlem.ustundag@iuc.edu.tr)

<sup>2</sup> Istanbul University-Cerrahpasa, Department of Civil Engineering, Istanbul (Türkiye), [celik@iuc.edu.tr](mailto:celik@iuc.edu.tr)

\*Correspondence: [ozlem.ustundag@iuc.edu.tr](mailto:ozlem.ustundag@iuc.edu.tr)

**Received:** 11.06.2021; **Accepted:** 01.08.2022; **Published:** 30.08.2022

**Citation:** Ozlem U. and Ozlem C.S. (2022). Effect of aerogel/silica fume under curing methods on properties of cement-based mortars. *Revista de la Construcción. Journal of Construction*, 21(2), 368-386. <https://doi.org/10.7764/RDLC.21.2.368>.

**Abstract:** In this study, the mechanical, thermal and porosity properties of mortar samples containing aerogel and silica fume under different curing conditions were investigated. For this purpose, 0%, 0.25% and 0.50% by weight of silica aerogel as a cement additive and 10% silica fume as an industrial waste material were incorporated in the cement mixtures. The prepared mortar samples were exposed to curing process in water, the wetting-drying effect and  $MgSO_4$  effect for 16 weeks. The highest thermal conductivity reduction of 31.2% was obtained from the water curing sample with silica fume addition at an aerogel content of 0.25%. Maximum compressive and flexural strengths were determined respectively from samples with silica fume addition at an aerogel content 0.50% as 74.5 MPa and no aerogel content as 11.3 MPa by wetting-drying curing. However, the lowest thermal conductivity coefficient was measured as 1.458 W/mK from the sample at an 0.25% aerogel content containing silica fume which completed the curing process under the influence of  $MgSO_4$  with a highest compressive strength increase by 24.6%.

**Keywords:** aerogel, silica fume, curing procedure, thermal conductivity, porosity.

## 1. Introduction

High energy consumption in buildings has made it necessary to take steps to ensure more durable environmental conditions and cost savings. However, the rapid decrease in natural resources reserves in the world reveals the necessity of restricting the use of natural resources in both production and heating stages. In addition, the need to reduce the increased  $CO_2$  emission due to global warming requires the limitation of fossil fuel use in buildings. From this point of view, the combination of technological materials and industrial waste materials offers a sustainable solution.

The most effective way to reduce energy losses in buildings is to improve thermal insulation in buildings (Saboktakin & Saboktakin, 2015). Instead of insulating buildings by covering them from the outside or inside, the use of aerogels with superior properties in providing insulation during the production of mortar has become an interesting issue day by day. Silica-based aerogels are very light and superior thermal insulating nano materials, consisting of more than 90% of air and the rest of silica. They have very large surface area, low density, low thermal conductivity and very small pores at nanometer (nm) level (Bostanci, 2020b; Feng et al., 2015; Gomes et al., 2018; Haranath et al., 1997; Ibrahim et al., 2015; Rao et al., 2005; Saboktakin & Saboktakin, 2015).

In studies where aerogel is used to improve the thermal insulation of cement-based mixtures, aerogel is used in large amounts instead of sand by volume (Fátima Júlio, Ilharco, et al., 2016; Fátima Júlio, Soares, et al., 2016; T. Gao et al., 2014; Ng et al., 2015; Ng, Jelle, & Stæhli, 2016; Ng, Jelle, Zhen, et al., 2016; Zaidi et al., 2019). However, the high cost of silica aerogel necessitates its use in small amounts in cement-based mixtures (Garrido et al., 2017; Ibrahim et al., 2015; Li et al., 2019; Z. Liu et al., 2016).

In one of the studies in which aerogel was used in a small amount, researchers examined the effect of the pore structure on the mechanical strength and thermal conductivity of the mortars under different curing conditions they produced at an aerogel content 0.1-1.0% by weight. The highest compressive strength of the samples cured in water was obtained as 57 MPa at an aerogel content 1.0%, 60.8 MPa and 44.3 MPa at an aerogel content 0.5% under the influence of wetting - drying and MgSO<sub>4</sub> curing conditions, respectively. The lowest thermal conductivity coefficient of mortars was obtained as 1.56 W/mK at an aerogel content 0.3% for water curing group, 1.80 W/mK at 0.3% aerogel loading for wet-drying curing group and 1.61 W/mK at 0.1 aerogel loading for MgSO<sub>4</sub> curing group (Bostancı et al., 2019).

Among the waste binders, silica fume is quite remarkable compared to other waste binders due to its superior contribution to the calcium-silicate structure (Liu et al., 2019). Silica fume particles are composed of much finer particles compared to cement particles and this provides faster chemical reaction and higher mechanical properties (Gesoglu et al., 2016; Schröfl et al., 2012). Demirboğa and Gül (2003), in their study to determine the effect of silica fume on the thermal conductivity of lightweight aggregate concrete, added 10, 20, 30% silica fume by weight to the mixtures as a partial replacement of cement. It has been determined that thermal conductivity decreases with the increasing silica fume ratio and there is a decrease up to 18.5% in thermal conductivity at a ratio of 30% silica fume. Demirboğa (2003) measured thermal conductivity and compressive strength by adding 10%, 20% and 30% silica fume by weight as a replacement of cement to the mixtures he prepared. It has been stated that in the mortars where 10%, 20% and 30% silica fume was added, the thermal conductivity decreased by 17%, 31% and 40%, respectively, with the increasing silica fume content. In mortars with a ratio of 10% silica fume content, there was a slight increase in the 120-days compressive strength, and it was observed that the compressive strength decreased in mixtures at a ratio of more than 10% silica fume.

Xu and Chung (2000) stated in their study that the thermal conductivity value of cement pastes and mortars to which silica fume was added decreased by 38% and the effects of silica fume addition on mortar and cement paste were in the same direction. Fu and Chung (1997) investigated the thermal conductivity of cement pastes prepared by adding 20-30% latex and 15% silica fume by cement weight, and they emphasized that the addition of silica fume is very effective in reducing thermal conductivity. Xu and Chung (1999) similarly prepared cement pastes using 15% silica fume and 0.5% carbon fiber by weight of cement in their study and stated that the addition of silica fume reduces thermal conductivity.

There are many studies in the literature that improve the thermal insulation properties of cement-based mixtures by adding high amounts of aerogel to the mixtures. On the other hand, aerogel is a high cost material. In the study carried out considering this situation i. It is aimed to reduce the thermal conductivity of the mixtures by using low amount of aerogel cement as additive material. ii. By adding a small amount of silica fume to the mixtures, it was tried to prevent the decreases in the compressive strength caused by the use of aerogel and the combined effect of aerogel and silica fume was investigated. iii. The mechanical, thermal and porosimetry properties of the mortars under different curing conditions were investigated. iv. The thermal conductivity properties of the mortars exposed to different curing conditions have been examined by considering the pore types in the mortars.

## 2. Materials and methods

### 2.1. Materials

CEM I 42.5 R type ordinary Portland cement and Standard Rilem sand used in mortar production were obtained from Limak Cement Inc. Cementitious material both cement and silica fume conform to the current specifications as described

in TS EN 197-1 (2012). The silica fume used as mineral additives was supplied from Antalya ferrochrom factory. Chemical and physical properties of the cement and silica fume used are given in Table 1.

The silica aerogel used to reduce the thermal conductivity of the mortar samples was purchased from Alison Aerogel Hong Kong. The properties of aerogel are presented in Table 2.

**Table 1.** Chemical and physical properties of used cement and silica fume.

Chemical composition (wt/wt%)	Cement	Silica fume	TS EN 197-1
SiO <sub>2</sub>	19.19	87.63	
Al <sub>2</sub> O <sub>3</sub>	4.71	0.72	
Fe <sub>2</sub> O <sub>3</sub>	3.03	0.29	
CaO	62.31	0.75	
MgO	2.41	3.95	
SO <sub>3</sub>	2.98	0.60	≤ 4.0
K <sub>2</sub> O	0.66	-	
Na <sub>2</sub> O	0.19	-	
Cl <sup>-</sup>	0.0095	-	≤ 0.1
Loss on ignition	3.65	2.59	
Insoluble residue	0.33	-	≤ 5.0
Total alkali	0.53	-	
C <sub>3</sub> A	7.29	-	
Physical properties			
Setting time (min.)	141		
	198		
Specific gravity (g/cm <sup>3</sup> )	3.03	2.29	
Specific surface area (cm <sup>2</sup> /g)	3755	230,000	

**Table 2.** Physical properties of silica aerogel.

Appearance (Color)	White
Surface area (m <sup>2</sup> /g)	750-850
Pore diameter (nm)	8-10
Porosity (%)	> 95
Apparent density (kg/m <sup>3</sup> )	90-100
Surface group	OH <sup>-</sup>

## 2.2. Mix proportions and preparing specimens

In order to determine the compressive strength, flexural strength, thermal conductivity and porosity properties of mortars cured under different conditions, mixture ratios with 4 different compositions were prepared. In the production of mortar specimens, silica fume at a fixed rate of 10% was used as a replacement of cement. Aerogel, which is used to reduce thermal conductivity, was added to the mortar mixtures at the ratio of 0, 0.25 and 0.50% by weight of binder material.

While preparing the mortar samples, firstly, a dry mixture containing cement, silica fume, standard sand and silica aerogel particles was prepared. Later, by adding water gradually to this dry mixture, it was ensured that all materials were homogeneously distributed. A water/binder ratio of 0.50 was adjusted for mortar mixtures. The total amount of cement and silica fume in the mixtures has been calibrated as the total binding material. The silica aerogel in the mixtures was used as a cement additive by weight.

After the mixing process was completed, standard three-cell stainless steel molds of 40 mm x 40 mm x 160 mm were used for the cement mortar samples, and compression was carried out to prevent segregation in the mixtures. Mortar specimens were taken out of the mold after waiting in the mold for 24 hours at room temperature ( $21 \pm 2^\circ \text{C}$ ) and 3 samples produced from each mixture were placed in different curing environments. The mixing ratios of the prepared mortar samples are presented in Table 3.

**Table 3.** Mixture proportions of silica fume and aerogel incorporated mortars.

Mixture no.	Cement content (%)	SF content (%)	Aerogel content (%)	Cement (g)	SF (g)	Aerogel (g)	Water/Cement	Water (ml)	Sand (g)
S1 (control)	100	0	0	450	0	0			
S2(10% SF)	90	10	0	405	45	0			
S3 (10% SF+ 0.25% Aerogel)	90	10	0.25	405	45	1.13	0.50	225	1350
S4 (10% SF+ 0.5% Aerogel)	90	10	0.50	405	45	2.25			

## 2.3. Curing methods

Three different curing environments are used for mortar mixtures. These are water curing, wetting-drying and  $\text{MgSO}_4$  curings. Three samples were prepared from each mixture for three different curing conditions and each mortar sample was cured in its own specific environment (Bostancı et al., 2019). For water curing, the mortars were kept in the curing pool at ( $21 \pm 2^\circ \text{C}$ ) for 16 weeks. Curing period was performed as recommended in the paper (Bostancı et al., 2019). Mortar samples cured under the effect of wetting-drying were kept in the curing pool at a temperature of  $21 \pm 2^\circ \text{C}$  for one week, and then kept at room temperature  $21 \pm 2^\circ \text{C}$  for the second week. The curing process was completed for 16 weeks with a wetting-drying cycle of 8 cycles in total. Samples that completed the curing process under the influence of  $\text{MgSO}_4$  were first kept in a solution containing 13%  $\text{MgSO}_4$  for one week, then in an oven at  $105^\circ \text{C}$  for one week. The curing process was carried out for a total of 8 cycles, one cycle of two consecutive weeks.

## 2.4. Testing

Mechanical tests were performed to the specimens that completed the 16-week curing processes in three different curing environments. In this context, firstly the flexural strength and compressive strength tests were applied to the samples, followed by thermal conductivity tests and mercury intrusion porosimetry tests (MIP).

The three-point flexural strength test was carried out to standard mortar specimens of  $40 \text{ mm} \times 40 \text{ mm} \times 160 \text{ mm}$ , with a middle span of 100 mm and a loading speed of  $50 \pm 10 \text{ N/s}$ . Flexural strength tests were applied to a total of three samples for each mixture. The flexural strength of the mixture was determined by considering the arithmetic average of the flexural strength of three samples.

After the flexural strength tests were performed to the mortar samples, the specimens were divided into two parts. The compressive strength test was carried out on the remaining 3 halves from the flexural strength tests. The specimens were loaded with a 40 mm × 40 mm contact surface. The applied compressive load in the experiment was adjusted to be 2400±100 N/s. The compressive strength of the samples was determined by considering the arithmetic mean of three measurements. Flexural strength and compressive strength tests were made in accordance with TS EN 1015-11 standard (TS EN, 2000).

Following the mechanical tests, thermal conductivity and MIP tests were performed. With the flexural strength test samples divided into two parts, the compressive strength test was applied on half of each sample. On the other half of the sample with the highest compressive strength, thermal conductivity test and then mercury intrusion porosimetry test (MIP) were carried out. Thermal conductivity coefficient measurements were made with TCi C-Therm device. This device measures the thermal conductivity coefficient of the specimens with the Modified Transient Plane Source (MTPS) method. The experiment was performed with five measurements taken from different parts of each sample. The thermal conductivity coefficient of the sample was determined by taking the average of these five measurements. With this device, thermal conductivity coefficient measurement can be made in a very short time such as 1-3 seconds for each sample. Thermal conductivity tests were carried out in accordance with ASTM D7984-16 standard (ASTM, 2016).

Mercury porosimetry tests were carried out on the samples after the thermal conductivity tests were performed. The pore structure properties of the mortar specimens can be determined with the mercury porosimetry test. Micromeritics brand device was used for this purpose. The device operates in the pressure range of 0.34 - 413.7 MPa and pore diameters in the range of 3-360,000 nm can be detected.

### 3. Results and discussion

#### 3.1. Compressive strength test results

The compressive strengths of the mortar samples cured in water and which completed the curing process under the influence of wetting-drying and MgSO<sub>4</sub> are presented in Figure 1. Firstly, when the effect of silica fume addition on the compressive strength for different curing conditions was examined, the compressive strength of the S2 sample containing 10% silica fume increased for wetting-drying and MgSO<sub>4</sub> environments compared to the S1 control specimen prepared with cement only. For the water curing medium, the compressive strength of the S2 sample with silica fume was reduced by 2.6% compared to the S1 control specimen. When the samples are evaluated according to their aerogel content; while 0.25% aerogel loading did not cause a significant change on the compressive strength in the water cured samples, the compressive strength decreased to 40.4 MPa by increasing the aerogel content from 0.25% to 0.50% and decreased by 30% compared to the S1 control sample.

For the wetting-drying cured samples, the 0.25% aerogel loading did not cause any change on the compressive strength (S2 and S3). However, with the increase of the aerogel inclusion ratio from 0.25% to 0.50%, there was an increase of 7.5% in compressive strength compared to the S1 control sample prepared with cement only.

For the samples exposed to MgSO<sub>4</sub> solution, a slight increase was observed in the compressive strength of the S3 sample with 0.25% aerogel loading compared to S2 without aerogel additive. In the case of increasing the aerogel inclusion ratio from 0.25% to 0.50% did not cause much change on the compressive strength (S3 and S4). The highest compressive strengths were seen in the samples that completed the curing process under the influence of wetting-drying. This is consistent with the literature (Bostancı et al., 2019). Using more than a certain content of aerogel as a cement additive in mortar mixtures causes additional gap formation and causes a decrease in compressive strength (Liu et al., 2016; Ng et al., 2015). However, since the silica fume is very fine grained, it reduces the permeability of the mortar in MgSO<sub>4</sub> and wetting-drying curing environments. For this reason, the reduction in compressive strength due to the use of aerogel is prevented. In water cured samples, 0.50% aerogel loading caused a serious decrease in compressive strength.

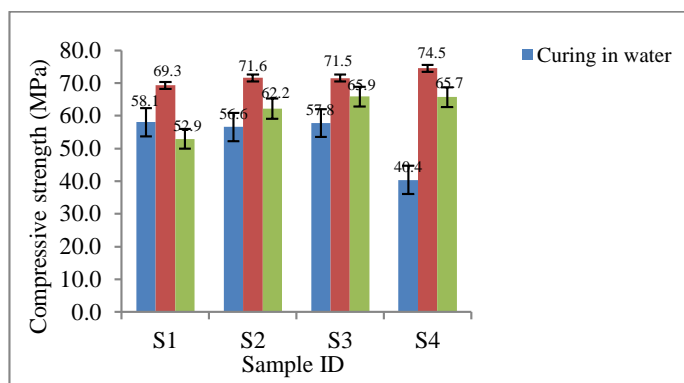


Figure 1. Compressive strength test results.

The correlation in Figure 2 represents the relationship between silica aerogel content and compressive strength for different curing conditions. It is seen that there is a good correlation with  $R^2$  of 0.99 between the silica aerogel content and the compressive strength on the samples that have completed their curing process in water. There is also a good agreement with the correlation coefficient  $R^2$  of 0.80 in the sample group which exposed to cycles of wetting-drying. The correlation coefficient between the aerogel content and the compressive strength in the samples that were cured in  $MgSO_4$  solution was slightly lower with  $R^2$  of 0.61. Among the samples cured in water, as the aerogel content increases the compressive strength decreases as expected. However, in the other two curing mediums the compressive strength tends to increase as the aerogel content increases.

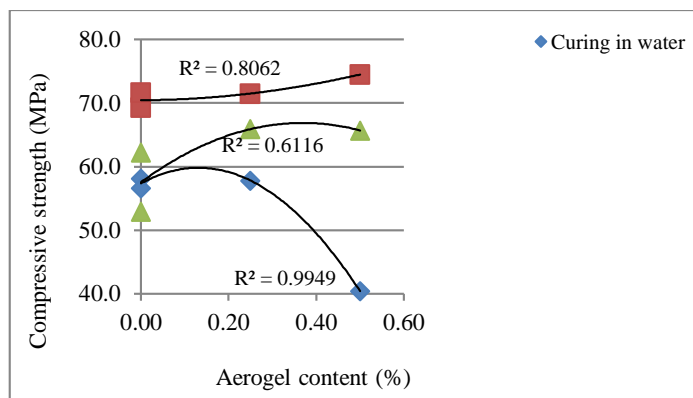


Figure 2. Silica aerogel content - compressive strength relationship.

### 3.2. Flexural strength test results

The flexural strength results of the mortars that were cured in water, wetting-drying and in  $MgSO_4$  solution are presented in Figure 3. When the samples without aerogel loading (S1 and S2) are evaluated, it can be stated that the S2 sample containing 10% silica fume does not have a significant change in the flexural strengths for all curing conditions compared to the S1 control sample prepared with cement. The flexural strengths of S1 and S2 samples exposed to wetting-drying curing and  $MgSO_4$  solution are 11.3 MPa and 10.0 MPa, respectively. While the flexural strength of the S1 sample cured in water and prepared with cement was 7.0 MPa, it was measured as 6.9 MPa for the sample S2 with the addition of 10% silica fume.

The flexural strengths of S2, S3 and S4 samples containing 10% silica fume are evaluated according to their aerogel content. Considering the samples that were completed the curing process in water, the flexural strength of the S3 sample

with 0.25% aerogel inclusion decreased by 20% compared to the S1 control sample. If the aerogel inclusion ratio is increased to 0.50%, an increase of 7% occurred in the flexural strength.

It was stated in previous studies that the sample with low aerogel content in the samples cured in water had the lowest flexural strength (Bostancı et al., 2019). 0.25% aerogel loading did not cause much change in the flexural strength of the mortars exposed to wetting-drying and MgSO<sub>4</sub> curing. In brief, the lowest flexural strength under the effect of MgSO<sub>4</sub> and wetting-drying curing was obtained from S4 samples with 0.50% aerogel inclusion and from S3 samples with 0.25% aerogel loading in the case of water curing.

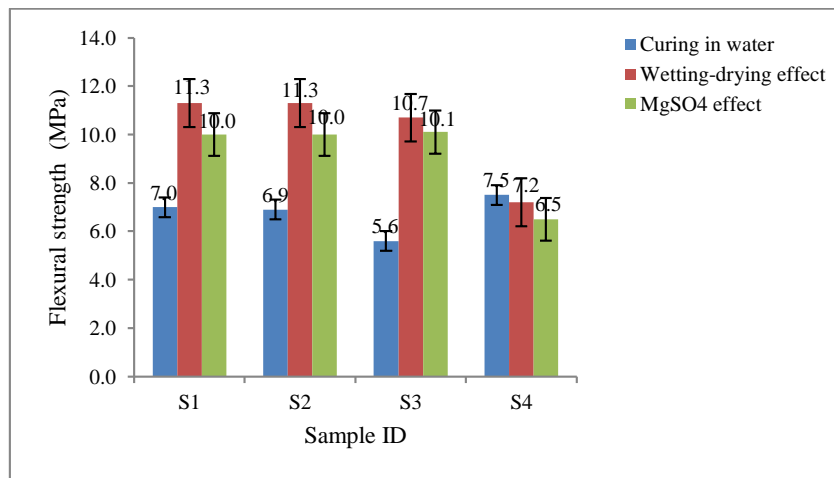


Figure 3. Flexural strength test results.

### 3.3. Thermal conductivity test results

The thermal conductivity coefficient results of the mortar samples that completed their curing process in water, under the influence of wetting-drying effect and MgSO<sub>4</sub> are presented in Figure 4. Considering the samples cured in water, the lowest thermal conductivity coefficient was obtained as 1.733 W/mK from the S3 sample containing 0.25% aerogel and 10% silica fume. The decrease in the thermal conductivity coefficient of the S3 sample compared to the control sample S1 prepared only with cement is on the order of 31%. The highest thermal conductivity coefficient in the case of water curing was obtained as 2.518 W/mK from the S1 control sample prepared with cement, without aerogel and silica fume. The decrease in the thermal conductivity of the S4 sample with 0.50% aerogel loading is 17.4% compared to the control sample. The change of thermal conductivity coefficient in samples that cured in water is compatible with the literature (Bostancı, 2020a; Bostancı & Sola, 2018; Bostancı et al., 2019). In these studies, it was stated that adding a small amount of aerogel to the mortar mixture is sufficient to reduce the thermal conductivity coefficient. In several studies, silica aerogel was added as partial replacement of sand by volume (Zaidi et al., 2020; Zaidi et al., 2019). In this study silica aerogel was used as a cement additive in the mixtures, that is why the expression “small amount” is used.

Among the samples that exposed to wetting-drying cycles, the lowest thermal conductivity coefficient was measured as 1.458W/mK from the sample S2 with 10% silica fume addition without aerogel additive. The thermal conductivity coefficient of this sample decreased by 22.4% compared to the S1 control sample. In the samples in this curing group, the highest thermal conductivity coefficient of 1.923 W/mK was obtained from S3 sample with 0.25% aerogel inclusion. Thermal conductivity coefficient of S3 sample increased by 2.3% compared to control sample S1. It can be said that in the wetting-drying curing group, aerogel loading has no effect on the decrease in thermal conductivity coefficient.

Among the samples that completed the curing process under the influence of MgSO<sub>4</sub>; it was determined that the thermal conductivity results of all samples containing silica fume were below the S1 control sample prepared with cement only. The thermal conductivity coefficient of the S2 sample with silica fume addition decreased by 5% compared to the S1

sample, while the thermal conductivity coefficient of S3 and S4 samples with 0.25% and 0.50% silica aerogel inclusion decreased by 7%, respectively. It can be said that the ratio of aerogel inclusion in this curing group does not have a significant reducing effect on the thermal conductivity coefficient. The lowest thermal conductivity coefficient was measured as 1.458 W/mK from S3 sample with 0.25% aerogel inclusion and S4 sample with 0.50% aerogel inclusion. Among all curing groups, the lowest thermal conductivity coefficients were obtained from samples that completed the curing process under the MgSO<sub>4</sub> effect.

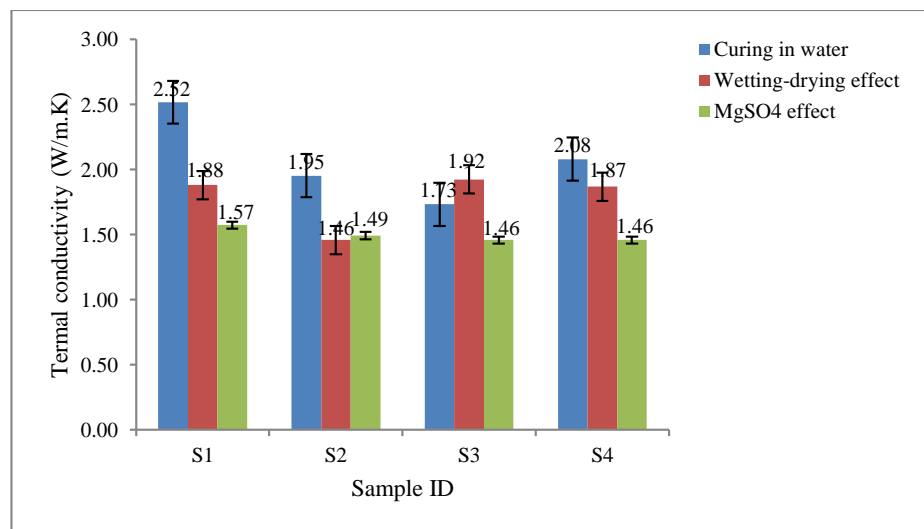


Figure 4. Thermal conductivity test results.

### 3.4. MIP test results

The pore structure of cement-based materials is effective on the mechanical and thermal properties of the materials. For this reason, being aware of the pore structure properties of the mortar samples such as mean pore diameter and pore size distribution is very important in terms of evaluating the mechanical and thermal properties of mortars (Bostanci, 2020a; Das & Kondraivendhan, 2012). In cement based materials, pore diameters can be measured in the range of nanometer to micrometer by mercury intrusion porosimetry test (Gao et al., 2016). MIP test results are given in Table 4.

Table 2. Physical properties of silica aerogel (a) water curing group, (b) wetting-drying curing group, (c) MgSO<sub>4</sub> curing group.

Mixture	Total porosity (%)	Median pore diameter - area (nm)	Average pore diameter (nm)	Total pore area (m <sup>2</sup> /g)
S1	12.39	14.10	40.20	5.772
S2	12.75	6.60	26.70	9.324
S3	12.20	5.10	16.50	14.059
S4	13.32	4.40	19.40	13.159

(b)				
Mixture	Total porosity (%)	Median pore diameter - area (nm)	Average pore diameter (nm)	Total pore area (m <sup>2</sup> /g)
S1	10.51	6.60	24.60	7.755
S2	11.15	4.60	18.30	11.410
S3	12.37	4.20	22.40	10.389
S4	12.25	3.10	19.80	11.524

(c)				
Mixture	Total porosity (%)	Median pore diameter - area (nm)	Average pore diameter (nm)	Total pore area (m <sup>2</sup> /g)
S1	13.61	17.00	71.00	3.640
S2	13.23	6.00	25.70	9.941
S3	12.50	6.40	26.10	9.236
S4	14.50	3.50	23.60	11.782

In the samples that cured in water, the total porosity of the S4 sample containing 0.50% aerogel with 10% silica fume addition has reached the highest value with 13.32%. The S4 sample is also the sample with the lowest compressive strength. This is consistent with other studies in the literature (Bostanci, 2020a; Bostanci et al., 2019). Median pore diameter-area (MPDA) and average pore diameter (APD) were significantly reduced by adding silica fume to the mixtures for this curing group. The MPDA decreased regularly with the addition of 0.25% and 0.50% aerogel to the samples to which containing 10% silica fume. While S1 sample prepared with cement only, had the highest APD, the lowest APD was obtained from the sample S3 with 0.25% aerogel inclusion. However, S3 sample in this curing group has the highest total pore area. In other words, while the MPDA and APD values decrease, the total pore area has the highest value. This situation explains that S3 has the lowest thermal conductivity coefficient among the samples that cured in water. S1 has the lowest total pore area and it is the sample with the highest thermal conductivity coefficient in water curing group.

In the samples that completed their curing process under the influence of wetting-drying, S1 sample prepared which was with cement only has the highest MPDA and APD. S1 is also the sample with the lowest compressive strength in this curing group. S2 sample containing 10% silica fume without aerogel and S4 sample with 0.50% aerogel loading are the two samples with the highest total pore area. However, the lowest thermal conductivity coefficient in this curing group was obtained from the S1 sample. At this point, it is thought that the median pore diameter area is determinant. The MPDA of S1 is greater than S4.

In the samples that have completed the curing process in the MgSO<sub>4</sub> solution, the S1 sample prepared with cement only is the sample with the highest MPDA and APD. S1 is also the sample with the lowest compressive strength. The APD values of S2, S3 and S4 samples containing silica fume and different proportions of aerogel, are close to each other and the thermal conductivity coefficients of these samples are also very close to each other. The total pore area values of these samples are also high. The S1 sample with the lowest total pore area is also the sample with the highest thermal conductivity coefficient in this curing group.

The relationship between the MDPDA and compressive strength of the samples under different curing conditions is shown in Figure 5. As mentioned before above, there is a good correlation between the compressive strength and MPDA of the mortar samples that have completed the curing process under the wetting-drying and MgSO<sub>4</sub> effect, with a correlation

coefficient  $R^2$  of 0.97 and 0.99, respectively. However, with the correlation coefficient  $R^2$  0.61, it can be stated that the median pore diameter area is not very effective on the compressive strength of the samples that are cured in water.

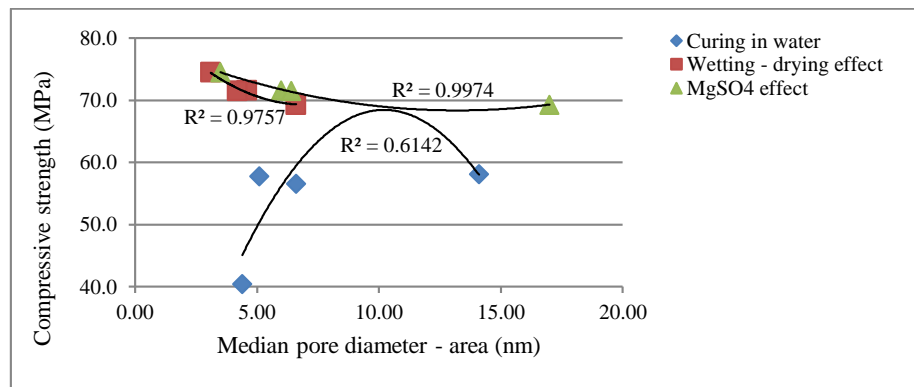


Figure 5. Relationship between the MPDA and compressive strength.

The relationship between the APD and the thermal conductivity coefficients of the samples that have completed the curing processes in water, under the effect of wetting-drying and  $MgSO_4$  solution are presented in Figure 6. There is a good correlation between the thermal conductivity and APD values of the mixtures for all curing conditions.

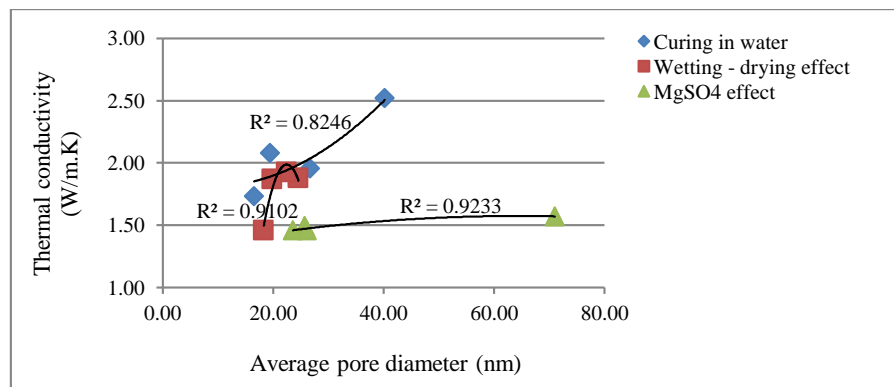
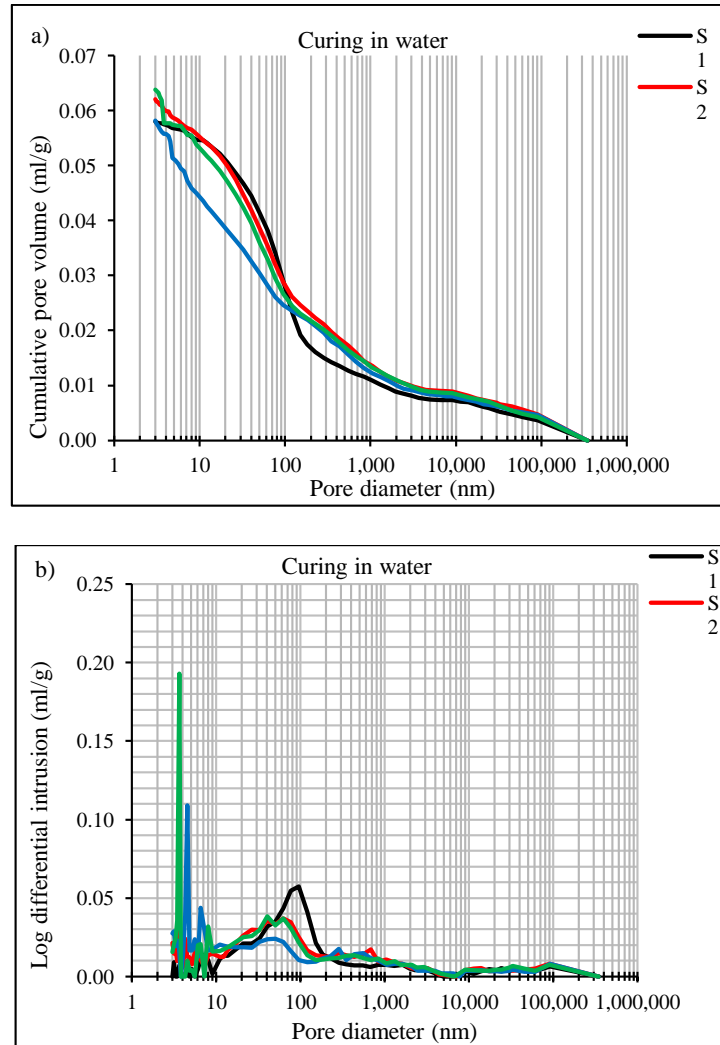


Figure 6. Relationship between THE APD and thermal conductivity.

The relationship between the pore diameter and the cumulative pore volume obtained from the mercury intrusion porosimetry test results is presented sequentially for 3 different curing mediums. In Figure 7, it is seen that the behavior of the samples cured in water changes after 100 nm. 100 nm becomes the critical diameter for pore diameter - cumulative pore volume curves.

On the other hand, when the differential intrusion curves of the samples are examined; it is seen that the S3 sample with 10% silica fume and 0.25% aerogel inclusion shows a significant increase in the 4-8 nm pore diameter range. The S3 sample is the sample with the lowest thermal conductivity coefficient with 1.733 W/mK in this curing group. As stated in previous studies, this size range corresponds to the average pore sizes of the aerogel used and this situation indicates the contribution of the aerogels to the development of the pore structure in the mortars (Bostanci, 2020a). At the same time, the apparent increase of the S3 sample in the 4-8 nm pore diameter range indicates that the pore type that is effective in determining the thermal conductivity of this sample is gel pores. Differential intrusion curves of all samples in the 4-8 nm size range are compatible with the thermal conductivity values. The pore volume corresponding to diameters smaller than 10 nm is closely related with the occurrence of hydration products (Cheng, 2012) For this reason, it can be stated that the low amount of aerogel additive such as 0.25% is effective in the formation of hydration products.

S4 sample containing 0.50% aerogel reached the highest values in differential intrusion curve at the range of 30,000 - 50,000 nm pore diameter. The S4 sample is the sample which has the lowest compressive strength. For samples that cured in water, it can be stated that the effective pore diameter range is 30,000-50,000 nm for determining the compressive strength.



**Figure 7.** Relationship between pore volume-pore diameters for water curing group.

Figure 8a shows the pore diameter - cumulative pore volume relationship of the samples which exposed to the wetting-drying curing. The behavior of the samples changes after 200 nm. 200 nm is the critical diameter for the cumulative pore volume curves.

When the differential intrusion curves of the samples are examined; the S2 sample with the addition of 10% silica fume has an apparent increase at the diameter range of 4-8 nm in differential intrusion curves. At the same time, S2 is the sample which has the lowest thermal conductivity coefficient with 1.458 W/mK. S1, S3 and S4 samples have proportional values in intrusion curves to their thermal conductivity coefficient in the range of 4-8 nm pore diameter. In summary, it can be stated that the pore type that is effective to determine the thermal conductivity for the samples cured under the effect of wetting-drying is gel pores.

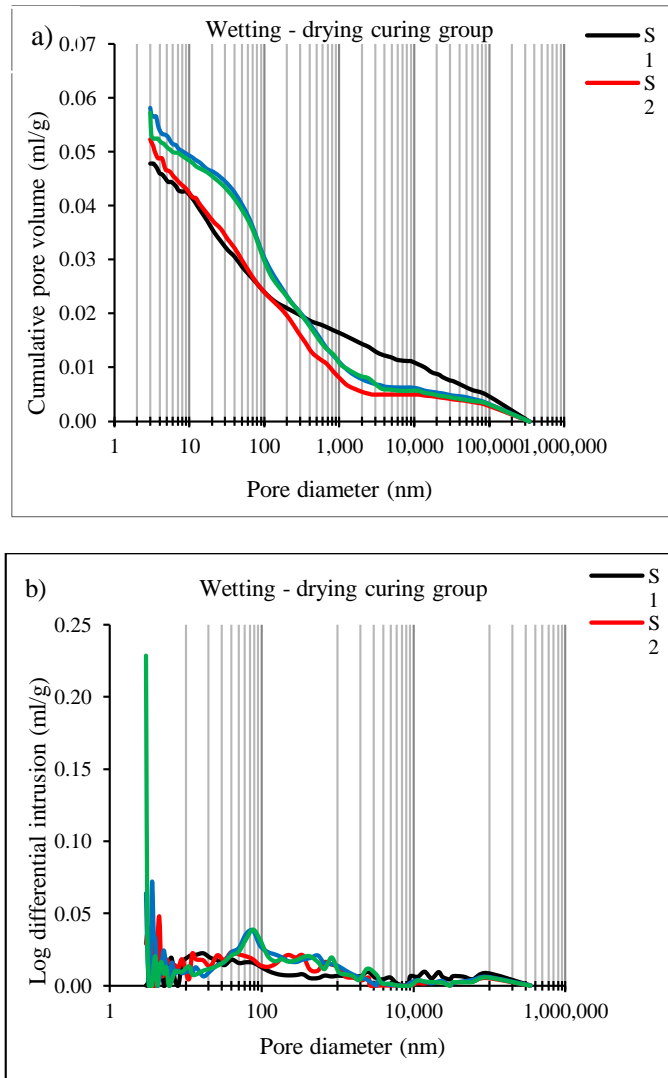


**Figure 8.** Relationship between pore volume-pore diameters for wetting-drying curing group.

The pore structure of the tests that completed the curing process under the  $MgSO_4$  effect is presented in Figure 9. When the cumulative pore volume curves are examined, it is seen that the behaviors of the samples change after 200 nm. 200 nm is the critical diameter for the cumulative pore curves of samples cured under  $MgSO_4$  effect.

When the differential intrusion curves of the samples are examined; the S1 sample with the highest thermal conductivity coefficient has an apparent decrease in pore sizes between 4-8 nm in differential intrusion curves. S2, S3 and S4 samples with lower thermal conductivity coefficients have higher differential intrusion values. The S1 sample has higher differential intrusion values at a pore diameter range  $>100,000$  nm, but S1 is also the sample which has the lowest compressive strength.

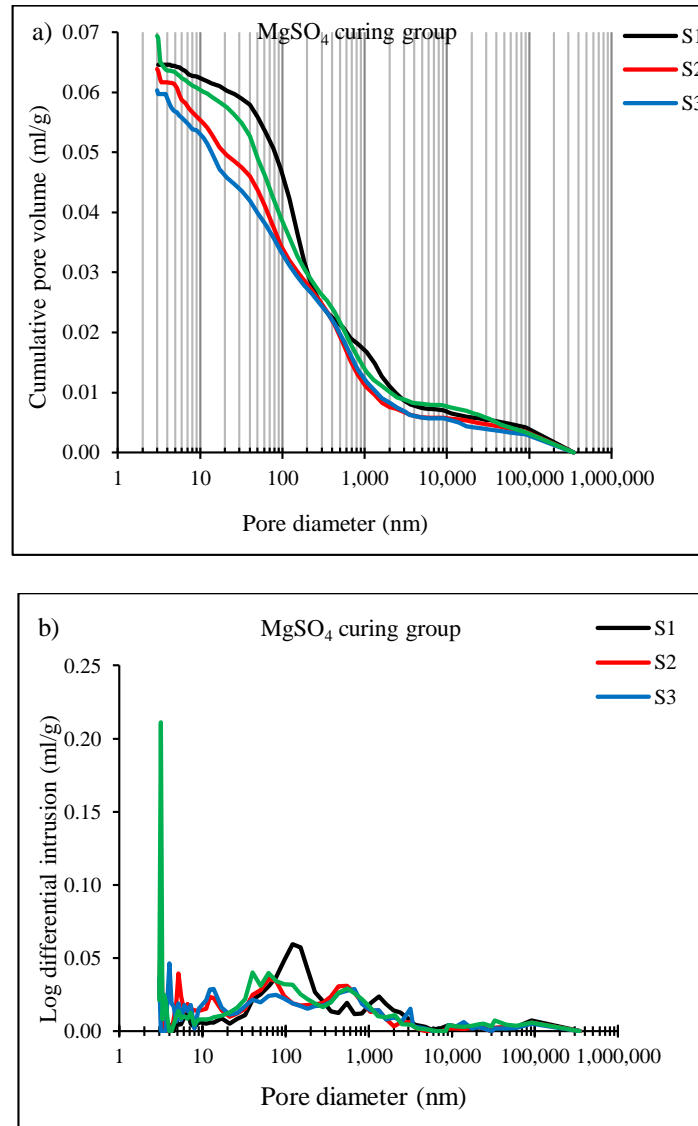


**Figure 9.** Relationship between pore volume-pore diameters for MgSO<sub>4</sub> curing group.

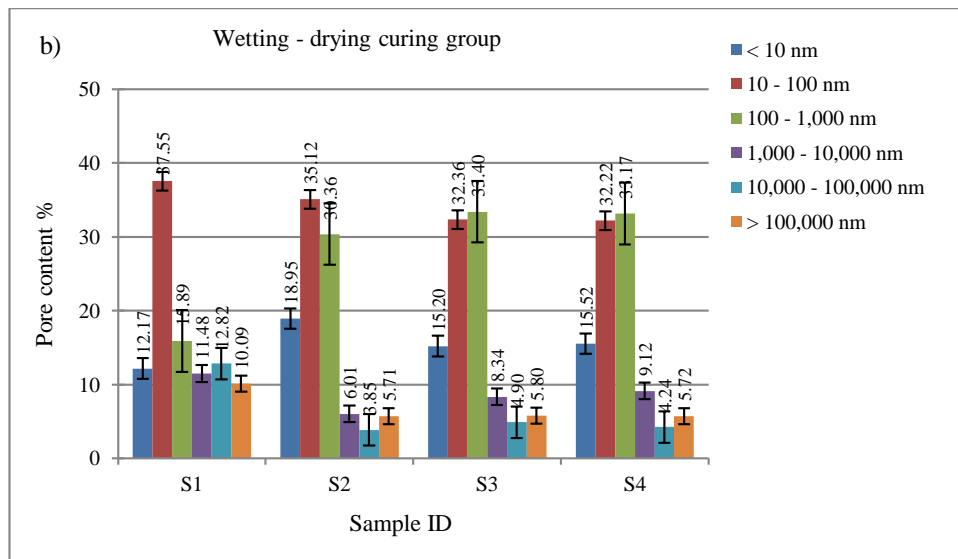
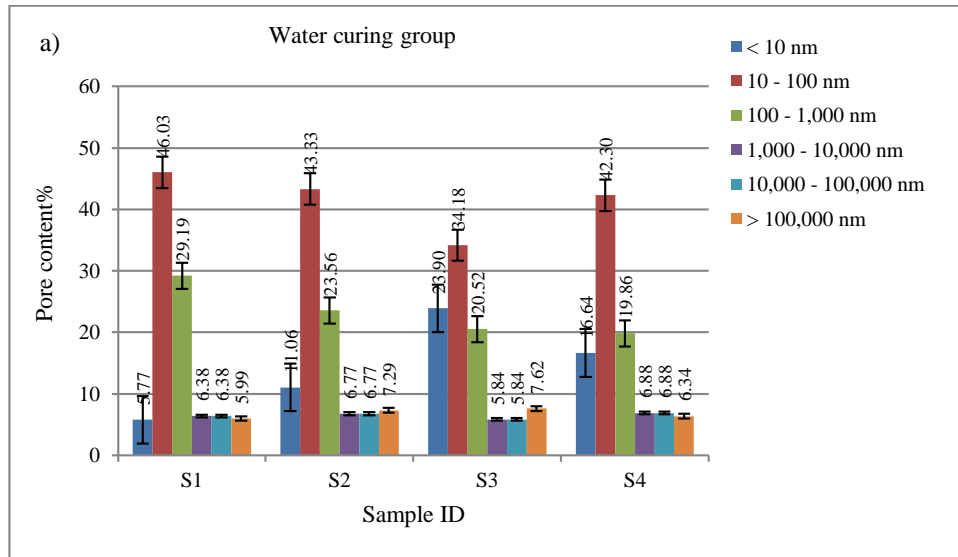
In cement-based materials, pores are categorized into three groups according to their size: gel pores, capillary pores and macro pores. Gel pores show pore diameter range <10 nm, capillary pores show 10-10,000 nm range, and macro pores show pore diameter range >10,000 nm (Dong et al., 2017).

Figure 10 shows the content of pores in pore structure of the mortar samples that completed the curing process in different environments. When the samples cured in water are examined, the gel pore level of S3 sample containing 0.25% aerogel inclusion shows a significant increase. S3 is also the sample which has the lowest thermal conductivity coefficient. As stated previously, it can be reiterated that the gel pore level is effective in determining thermal conductivity of samples cured in water.

Among the samples that exposed to the wetting-drying curing, the lowest thermal conductivity coefficient was obtained from the S2 sample containing 10% silica fume without aerogel additive. In Figure 8b, it is seen that the gel pore content of S2 sample is higher than all other samples. As stated before, it is seen that the gel pore content is effective in determining the thermal conductivity of the samples cured under the influence of wetting-drying. It was determined from the differential

intrusion curves of the samples that pore diameters >9,000 nm were effective in the compressive strength. This is confirmed when the pore content of the S1 sample with the lowest compressive strength is examined.

The gel pores content at the pore diameter range <10 nm of the S1 sample, which has the highest thermal conductivity coefficient, is at the lowest level among the samples that completed the curing process under the influence of MgSO<sub>4</sub> effect. S1 sample is also the sample with the lowest compressive strength in this cure group. It was stated above that pore diameters >100,000 nm are effective in compressive strength. This situation overlaps with the pore content of the samples. Large diameters are effective in the compressive strength.



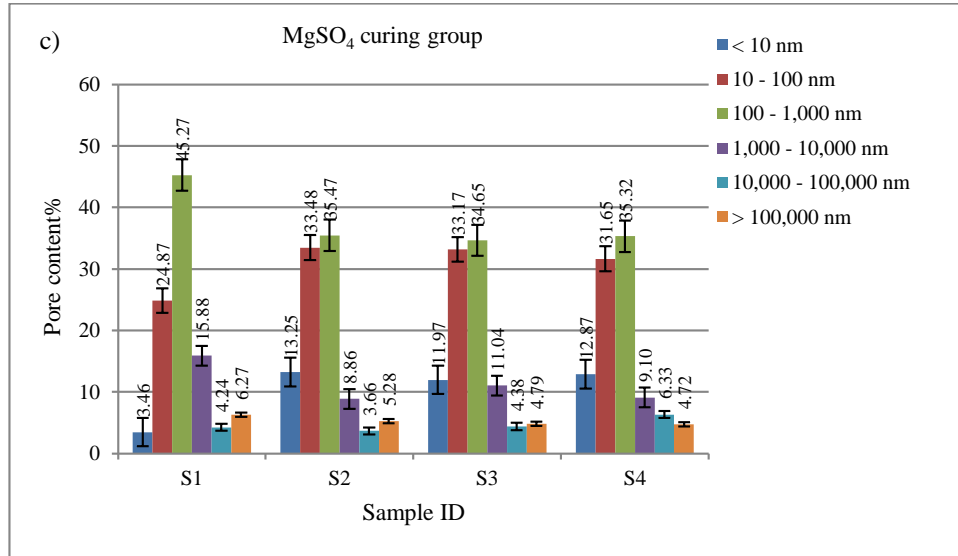


Figure 10. The fractions of total pore volume.

Figure 11 shows the relationship between the thermal conductivity coefficient and critical pore content of the samples that completed the curing process in water, under the wetting-drying and MgSO<sub>4</sub> effect. There is a good correlation with R<sup>2</sup> of 0.78 between the pore content at the range of <10 nm and the thermal conductivity coefficients of samples cured in water. In samples cured under the wetting-drying and MgSO<sub>4</sub> effect, the pore content at the range of <10 nm is effective in the estimation of thermal conductivity with the correlation coefficients of R<sup>2</sup> of 0.99 and 0.96, respectively. As stated before, gel pores are effective in determining thermal conductivity.

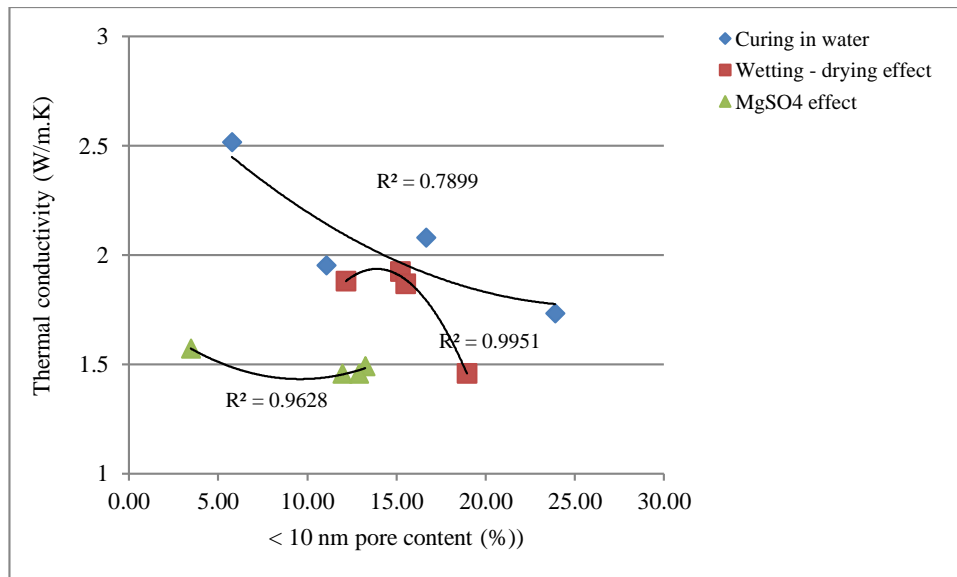


Figure 11. Thermal conductivity.

#### 4. Conclusions

In this study, the effects of using small amounts of aerogel and silica fume were investigated on the samples that completed their curing process in water, under the influence of wetting-drying and  $MgSO_4$ , and the following results were obtained.

##### Evaluation of compressive strength test results:

1. With the addition of silica fume to the mixtures, the compressive strength of the samples cured in wetting-drying and  $MgSO_4$  environments increased, and the compressive strength of the samples cured in water decreased;
2. While the 0.25% aerogel additive did not have an effect on the compressive strength in the samples that cured in water, the compressive strength decreased by 30.5% by increasing the aerogel additive ratio from 0.25% to 0.50%;
3. The use of 0.25% aerogel additive in the samples cured under the influence of wetting-drying did not cause any change in the compressive strength. With the increase of aerogel content from 0.25% to 0.50%, a 7.5% increase was observed in compressive strength compared to the reference sample;
4. While the compressive strength increased by 24.6% compared to the reference sample with the addition of 0.25% aerogel in the samples that completed the curing process under the influence of  $MgSO_4$ , increasing the aerogel additive rate to 0.50% did not have any effect on the compressive strength.

##### Evaluation of flexural strength test results:

1. It can be stated that the addition of silica fume to the mixtures does not have any significant effect on the flexural strength of the samples under different curing conditions;
2. While 0.25% aerogel inclusion caused a decrease in flexural strength for samples cured in water, an increase in flexural strength was observed when the aerogel content was increased from 0.25% to 0.50%;
3. Flexural strength of samples exposed to wetting-drying cycles and  $MgSO_4$  solution have shown similar behavior for 0.25% and 0.50% aerogel contribution. 0.25% aerogel inclusion did not cause any significant change in the flexural strength. However, a decrease in flexural strength was observed with the increase of aerogel content from 0.25% to 0.50%. The highest flexural strength values were obtained from samples cured under the influence of wetting-drying.

##### Evaluation of thermal conductivity - pore structure results:

1. For the samples that were under the influence of different curing conditions, the highest reduction in thermal conductivity by 31.2% was obtained in the water-cured sample containing 0.25% aerogel additive and 10% silica fume. No further reduction in thermal conductivity was observed when aerogel content was greater than 0.25%;
2. Among all curing groups, the highest thermal conductivity coefficients were obtained from samples cured in water, while the lowest thermal conductivity coefficients were obtained from samples that completed their curing process under the influence of the  $MgSO_4$  solution. By adding 10% silica fume to the mortar mixtures, reduction in thermal conductivity was achieved in all curing groups;
3. For samples cured under the influence of wetting-drying and  $MgSO_4$ , the use of 0.25% and 0.50% aerogel as cement additive did not have any significant effect on the reduction of thermal conductivity. For wet-drying and  $MgSO_4$  curing environments, if silica aerogel is used at low rates to provide thermal insulation, adding 10% silica fume to the mortar

mixes did not yield positive results in reducing thermal conductivity. In these conditions, it can be stated that silica fume is not a suitable mineral additive material in order to provide thermal insulation;

4. Pore volume corresponding to 4-8 nm pore diameter range is effective in determining thermal conductivity for all curing conditions. By adding silica fume to the mixtures, thermal conductivity control was brought to the level of gel pore;
5. For all curing groups, pore volume with large pore diameters has an influence on the compressive strength. For all curing groups, pore volume with large pore diameters has an influence on the compressive strength of the specimens. Pore volume at following ranges of pore diameters are decisive on the compressive strength:

Specimens with pore diameter between 30,000 nm and 50,000 nm cured in water,  
Specimens with pore diameter >9,000 nm cured under the influence of wetting-drying.  
Specimens with pore diameter >100,000 nm cured under the influence of MgSO<sub>4</sub>.

In order to improve the insulation feature in buildings, the combined use of small amounts of nano-technological and waste-based materials gives positive results for cement-based materials cured in water. It is an economical solution for traditional water curing method to reduce energy losses without decreasing their compressive strength, by using small amounts of silica aerogels which have high cost. On the other hand, it is possible to reduce the thermal conductivity of hybrid mortars exposed to wetting-drying cycles by using a small amount of waste material.

**Author contributions:** Each author contributed to the design and implementation of the study, to the analysis of the results and writing of the manuscript.

**Funding:** This study was supported by the Istanbul University-Cerrahpaşa, Scientific Research Unit, PhD dissertation project titled “Porosity properties of cement mortars with mineral additive cured in durabil medium” with the number 33536.

**Acknowledgments:** The authors specially thank Head of Limak Cement Yenibosna Concrete Inc.

**Conflicts of interest:** The authors declare no conflict of interest.

## References

- ASTM. (2016). *Standard Test Method for Measurement of Thermal Effusivity of Fabrics Using a Modified Transient Plane Source (MTPS) Instrument*. ASTM International West Conshohocken, PA, USA.
- Bostanci, L. (2020a). A comparative study of petroleum coke and silica aerogel inclusion on mechanical, pore structure, thermal conductivity and micro-structure properties of hybrid mortars. *Journal of Building Engineering*, 31, 101478. <https://doi.org/https://doi.org/10.1016/j.jobee.2020.101478>
- Bostanci, L. (2020b). Synergistic effect of a small amount of silica aerogel powder and scrap rubber addition on properties of alkali-activated slag mortars. *Construction and Building Materials*, 250, 118885. <https://doi.org/https://doi.org/10.1016/j.conbuildmat.2020.118885>
- Bostanci, L., & Sola, O. C. (2018). Mechanical Properties and Thermal Conductivity of Aerogel-Incorporated Alkali-Activated Slag Mortars. *Advances in Civil Engineering*, 2018. <https://doi.org/10.1155/2018/4156248>
- Bostanci, L., Ustundag, O., Sola, O. C., & Uysal, M. (2019). Effect of various curing methods and addition of silica aerogel on mortar properties. *Gradjevinar*, 71(8), 651–661. <https://doi.org/10.14256/JCE.2469.2018>
- Cheng, A. (2012). Effect of incinerator bottom ash properties on mechanical and pore size of blended cement mortars. *Materials & Design (1980-2015)*, 36, 859–864. <https://doi.org/https://doi.org/10.1016/j.matdes.2011.05.003>
- Das, B. B., & Kondraivendhan, B. (2012). Implication of pore size distribution parameters on compressive strength, permeability and hydraulic diffusivity of concrete. *Construction and Building Materials*, 28(1), 382–386. <https://doi.org/https://doi.org/10.1016/j.conbuildmat.2011.08.055>
- Demirboğa, R. (2003). Influence of mineral admixtures on thermal conductivity and compressive strength of mortar. *Energy and Buildings*, 35(2), 189–192. [https://doi.org/https://doi.org/10.1016/S0378-7788\(02\)00052-X](https://doi.org/https://doi.org/10.1016/S0378-7788(02)00052-X)

- Demirboğa, R., & Gül, R. (2003). The effects of expanded perlite aggregate, silica fume and fly ash on the thermal conductivity of lightweight concrete. *Cement and Concrete Research*, 33(5), 723–727. [https://doi.org/https://doi.org/10.1016/S0008-8846\(02\)01032-3](https://doi.org/https://doi.org/10.1016/S0008-8846(02)01032-3)
- Dong, H., Gao, P., & Ye, G. (2017). Characterization and comparison of capillary pore structures of digital cement pastes. *Materials and Structures*, 50(2), 154. <https://doi.org/10.1617/s11527-017-1023-9>
- Fátima Júlio, M., Ilharco, L. M., Soares, A., Flores-Colen, I., & de Brito, J. (2016). Silica-based aerogels as aggregates for cement-based thermal renders. *Cement and Concrete Composites*, 72, 309–318. <https://doi.org/10.1016/j.cemconcomp.2016.06.013>
- Fátima Júlio, M., Soares, A., Ilharco, L. M., Flores-Colen, I., & de Brito, J. (2016). Aerogel-based renders with lightweight aggregates: Correlation between molecular/pore structure and performance. *Construction and Building Materials*, 124, 485–495. <https://doi.org/https://doi.org/10.1016/j.conbuildmat.2016.07.103>
- Feng, J., Xiao, Y., Jiang, Y., & Feng, J. (2015). Synthesis, structure, and properties of silicon oxycarbide aerogels derived from tetraethylortosilicate /polydimethylsiloxane. *Ceramics International*, 41(4), 5281–5286. <https://doi.org/https://doi.org/10.1016/j.ceramint.2014.11.111>
- Fu, X., & Chung, D. D. L. (1997). Effects of Silica Fume, Latex, Methylcellulose, and Carbon Fibers on The Thermal Conductivity and Specific Heat of Cement Paste. In *Cement and Concrete Research* (Vol. 27, Issue 12).
- Gao, T., Jelle, B. P., Gustavsen, A., & Jacobsen, S. (2014). Aerogel-incorporated concrete: An experimental study. *Construction and Building Materials*, 52, 130–136. <https://doi.org/https://doi.org/10.1016/j.conbuildmat.2013.10.100>
- Gao, Y., Wu, K., & Jiang, J. (2016). Examination and modeling of fractality for pore-solid structure in cement paste: Starting from the mercury intrusion porosimetry test. *Construction and Building Materials*, 124, 237–243. <https://doi.org/https://doi.org/10.1016/j.conbuildmat.2016.07.107>
- Garrido, R., Silvestre, J. D., & Flores-Colen, I. (2017). Economic and Energy Life Cycle Assessment of aerogel-based thermal renders. *Journal of Cleaner Production*, 151, 537–545. <https://doi.org/https://doi.org/10.1016/j.jclepro.2017.02.194>
- Gesoglu, M., Güneyisi, E., Asaad, D. S., & Muhyaddin, G. F. (2016). Properties of low binder ultra-high performance cementitious composites: Comparison of nanosilica and microsilica. *Construction and Building Materials*, 102, 706–713. <https://doi.org/10.1016/J.CONBUILDMAT.2015.11.020>
- Gomes, M. G., Flores-Colen, I., da Silva, F., & Pedroso, M. (2018). Thermal conductivity measurement of thermal insulating mortars with EPS and silica aerogel by steady-state and transient methods. *Construction and Building Materials*, 172, 696–705. <https://doi.org/https://doi.org/10.1016/j.conbuildmat.2018.03.162>
- Haranath, D., Wagh, P. B., Pajonk, G. M., & Rao, A. V. (1997). Influence of sol-gel processing parameters on the ultrasonic sound velocities in silica aerogels. *Materials Research Bulletin*, 32(8), 1079–1089. [https://doi.org/https://doi.org/10.1016/S0025-5408\(97\)00086-X](https://doi.org/https://doi.org/10.1016/S0025-5408(97)00086-X)
- Ibrahim, M., Biwole, P. H., Achard, P., Wurtz, E., & Ansart, G. (2015). Building envelope with a new aerogel-based insulating rendering: Experimental and numerical study, cost analysis, and thickness optimization. *Applied Energy*, 159, 490–501. <https://doi.org/https://doi.org/10.1016/j.apenergy.2015.08.090>
- Li, P., Wu, H., Liu, Y., Yang, J., Fang, Z., & Lin, B. (2019). Preparation and optimization of ultra-light and thermal insulative aerogel foam concrete. *Construction and Building Materials*, 205, 529–542. <https://doi.org/https://doi.org/10.1016/j.conbuildmat.2019.01.212>
- Liu, Y., Shi, C., Zhang, Z., & Li, N. (2019). An overview on the reuse of waste glasses in alkali-activated materials. *Resources, Conservation and Recycling*, 144, 297–309. <https://doi.org/10.1016/J.RESCONREC.2019.02.007>
- Liu, Z., Ding, Y., Wang, F., & Deng, Z. (2016). Thermal insulation material based on SiO<sub>2</sub> aerogel. *Construction and Building Materials*, 122, 548–555. <https://doi.org/https://doi.org/10.1016/j.conbuildmat.2016.06.096>
- Ng, S., Jelle, B. P., Sandberg, L. I. C., Gao, T., & Wallevik, Ó. H. (2015). Experimental investigations of aerogel-incorporated ultra-high performance concrete. *Construction and Building Materials*, 77, 307–316. <https://doi.org/https://doi.org/10.1016/j.conbuildmat.2014.12.064>
- Ng, S., Jelle, B. P., & Stæhli, T. (2016). Calcined clays as binder for thermal insulating and structural aerogel incorporated mortar. *Cement and Concrete Composites*, 72, 213–221. <https://doi.org/https://doi.org/10.1016/j.cemconcomp.2016.06.007>
- Ng, S., Jelle, B. P., Zhen, Y., & Wallevik, Ó. H. (2016). Effect of storage and curing conditions at elevated temperatures on aerogel-incorporated mortar samples based on UHPC recipe. *Construction and Building Materials*, 106, 640–649. <https://doi.org/https://doi.org/10.1016/j.conbuildmat.2015.12.162>
- Rao, A. P., Rao, A. V., & Pajonk, G. M. (2005). Hydrophobic and physical properties of the two step processed ambient pressure dried silica aerogels with various exchanging solvents. *Journal of Sol-Gel Science and Technology*, 36(3), 285–292. <https://doi.org/10.1007/s10971-005-4662-1>
- Saboktakin, A., & Saboktakin, M. R. (2015). Improvements of reinforced silica aerogel nanocomposites thermal properties for architecture applications. *International Journal of Biological Macromolecules*, 72, 230–234. <https://doi.org/https://doi.org/10.1016/j.ijbiomac.2014.08.024>
- Schröfl, C., Gruber, M., & Plank, J. (2012). Preferential adsorption of polycarboxylate superplasticizers on cement and silica fume in ultra-high performance concrete (UHPC). *Cement and Concrete Research*, 42(11), 1401–1408. <https://doi.org/10.1016/J.CEMCONRES.2012.08.013>
- TS EN. (2000). Mortar Testing Method, Part 11. *Measurement of Compressive and Flexural Tensile Strength of Mortar*.
- Xu, Y., & Chung, D. D. L. (1999). Increasing the specific heat of cement paste by admixture surface treatments. In *Cement and Concrete Research* (Vol. 29).

- Xu, Y., & Chung, D. D. L. (2000). Effect of sand addition on the specific heat and thermal conductivity of cement. In *Cement and Concrete Research* (Vol. 30).
- Zaidi, A., Demirel, B., & Atis, C. D. (2019). Effect of different storage methods on thermal and mechanical properties of mortar containing aerogel, fly ash and nano-silica. *Construction and Building Materials*, 199, 501–507. <https://doi.org/10.1016/j.conbuildmat.2018.12.052>
- Zaidi, I. K., Demirel, B., Atis, C. D., & Akkurt, F. (2020). Investigation of mechanical and thermal properties of nano SiO<sub>2</sub>/hydrophobic silica aerogel co-doped concrete with thermal insulation properties. *Structural Concrete*, 21(3), 1123–1133. <https://doi.org/10.1002/suco.201900324>



Copyright (c) 2022 Ozlem U. and Ozlem C.S. This work is licensed under a [Creative Commons Attribution-Noncommercial-No Derivatives 4.0 International License](https://creativecommons.org/licenses/by-nc-nd/4.0/).